Established Technical Baseline
WP1320

UNIVERSITY OF BIRMINGHAM

Daniel White & Mike Antoniou

17th July 2024

Contents

1 Document Purpose

This document establishes the technical baseline for the passive radar system as part of the *"Aircraft Detection System for Optical Ground Stations"* project.

2 Introduction

Passive Coherent Location (PCL) is a radar technique that allows air surveillance without transmitting any signals. It relies on external sources of electromagnetic (EM) radiation, termed as Illuminators of Opportunity (IoO), to provide the illumination of targets so that their backscatter towards the passive radar can be measured and declared if detectable amongst the system noise. Longer range detection is possible with low frequency signals emitted by IoO, although this is highly dependent of target size. These signals are usually abundantly available in residential areas in the form of TV (DVB-T) signals.

Passive radar is advantageous in a few regards compared to active radar detection. As signal transmission (and therefore a high-power transmitter head) is not required, the ease of implementation is much greater, and adjustments to the system after the initial implementation are much simpler. Passive radar if using Digital TV or Radio IoO's makes the required components for implementation (discussed in Sec. 3) largely Commercial Off-The-Shelf (CotS) components that are readily available. PCL not transmitting, means there is no concern of spectral congestion or permissions required for operation. Additionally, common PCL frequencies such as DVB-T are licensed, which allows reliable operation in areas with high levels of transmission, without mutual interference.

Passive radar in exchange for these benefits may face potential issues not present for active systems. A non-cooperative transmitter requires efforts to validate a deployment through a site measurement, especially when some details of the IoO are not publicly or privately available. For a given site location, the IoO signal strength and quality are dependent on the transmitter type, power and the local geography. Generally, careful antenna placement and tuning is required to maximise the received (direct) signal strength to allow the extraction of target signals from the IoO backscatter. Thus, the theoretical maximum operating range could be shortened.

The following sections provide a broad overview of the hardware (Sec. 3), signal processing (Sec. 4) and details of the deployment site (Sec. 5) that will inform the anticipated operational capabilities with budget and time frame of this project.

3 Hardware Requirements

Four hardware components can broadly be used to build a passive radar system:

- Software Defined Radio (SDR) / Universal Software Radio Peripheral (USRP) device
- Band Pass Filter (BPF)
- Low-Noise Amplifier (LNA)
- Receiving Antennas

The hardware arrangement and required signal processing are shown in Figure 3. This section will describe the requirements for the radar hardware (left). Later, Section 4 will detail the processing steps (right) and enabling hardware requirements to perform target detection.

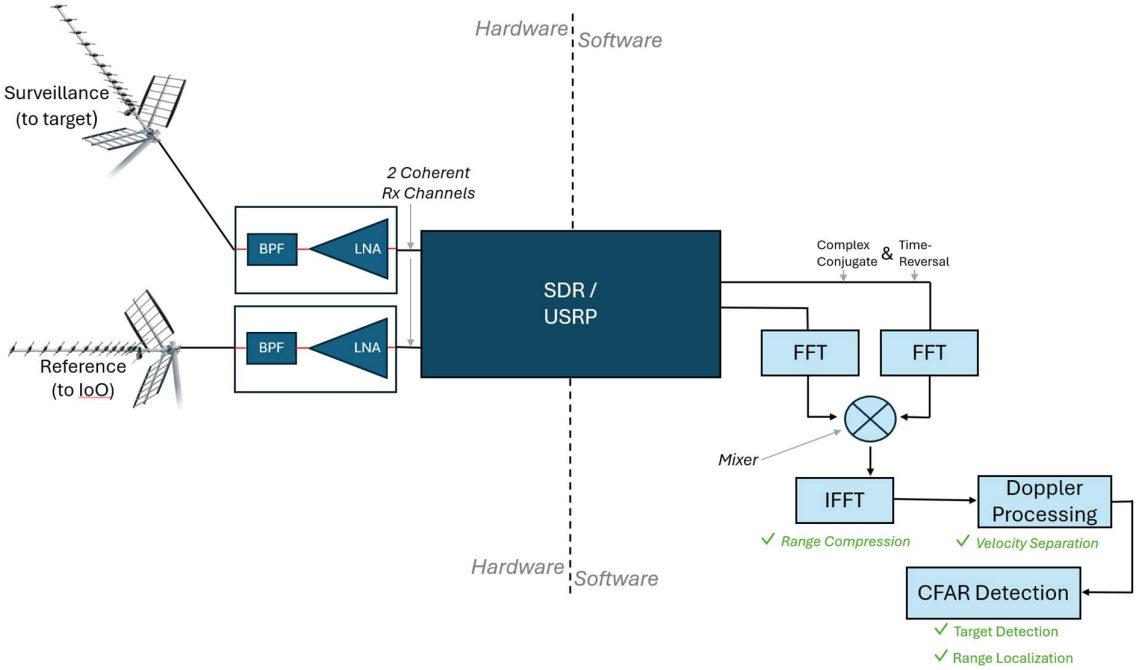

Figure 3 – Hardware Assembly and Signal Processing

3.1 USRP / SDR

A software defined radio is required to interrogate the passive signals for target detection. The features that are a requirement for passive radar is:

1. 2 Coherent Channels
   One for the *reference* channel, with an antenna pointed towards the transmitter, and another for the *surveillance* channel, with an antenna pointed towards the target area.

2. Coherent Processing
   At the UHF region (300MHz – 1 GHz), where PCL enabling signals have their centre frequencies. How received signals are coherently down-converted from their carrier frequency to baseband by the USRP is shown in Sec. 4.1.1.

3. >16MHz Bandwidth
   DVB-T with a single-channel bandwidth of 8MHz, requires at least double this to adequately sample echoes.

4. ADC 12-bits (minimum)
   As we will be working with both faint target echoes and direct signals from highly powered transmitters, there is a very high dynamic range of signals to be captured. The greater bit depth, the better we can avoid saturation of the Analogue to Digital Converters (ADCs).

Some options of SDRs suitable for the application are shown in Table 3.1-1 below.

Table 3.1-1 – USRP Options

Device Name	Company	Price (£1000, Approx.)	Esti. Manu. Lead Time	Technical Specification							URL
				Freq. Range (Hz)	Instant. Bandwidth	# Rx Chan.	Max Rx Gain (dB)	ADC depth	Noise Figure	Power Cons.	
USRP X410	Nat. Inst.	26.6	5wk	1M-7.2G	1.6G	4	~45	12	8dB	>190W	USRP X410 (Farnell)
USRP X440	Nat. Inst.	23.3	6wk	30M-4G	1.6G	8		12		>190W	USRP X440 (Farnell)
USRP-2955	Nat. Inst.	21.2	+8wk	10M-6G	80M	4	95dB	14	<5dB	~41W	USRP-2955 (Farnell)
USRP-2945	Nat. Inst.	19.0	11 wk	10M-6G	80M	4	95dB	14	<5dB	~41W	USRP-2945 (Digi-Key)
USRP-2954R	**Nat. Inst.**	**15.7**	**9 wk***	**10M-6G**	**160M**	**2**	**37.5dB**	**14**	**~6dB**	**~42W**	USRP-2954R (Farnell)
USRP-2944R	Nat. Inst.	13.8	9 wk*	10M-6G	160M	2	37.5dB	16	~6dB	~42W	USRP-2944R (Farnell)
USRP-2922	Nat. Inst.	-	No Longer Manufactured	400M-4.4G	>~20M	2	31.5dB	14	7	<18W	USRP-2922 (Farnell)

The USRP-2954R was selected as a flexible and reasonably cost-effective solution within the budget available. The manufacturer specifications are found here at ni.com. It was ordered, has arrived, and is pictured in Figure 3.1, with relevant specifications for PCL additionally shown in Table 3.1-2.

Figure 3.1 – USRP-2954R device pictured. Left, front panel; right, back panel

Table 3.1 – Key USRP2954(R) Specifications for PCL

Specification Parameter	Value	Comment
# Receiver Channels	2	2 is minimum required for PCL
Frequency Range	10 MHz - 6 GHz	For long range detection, <1GHz is most suitable.
Instantaneous Bandwidth	160MHz	DVB-T BW is 7MHz, DAB is 1.5MHz
Max. I/Q Sample Rate	200 MS/s	
ADC Resolution	14 bits	To deal with the large dynamic range of signals (bright and weak) associated with PCL measurements. Higher resolution also leads to less quantisation error, leading to phase errors and thus loss with coherent processing.
Max. Receiver Input Power	-15 dBm	10^{-5} W = 0.01mW
# Transmit Channels	2	Not going to be used for a passive setup

3.2 Band Pass Filter (BPF)

The band pass filter is used for both channels of the system to remove out of band interference in the receive chain. For PCL, this is doubly relevant as our receivers will be subject to other bright transmitter sources which could also increase the risk of saturation if these signals are not filtered out.

Bandpass filters are readily available at common radio frequency bands, such as at DVB-T, DAB or FM. To maximise the effectiveness of the filter used, it would be important to capture the signals received at the site and determine their frequency range, in order to buy the appropriate filter.

For DVB-T, Table 3.2 displays some candidate filters that could be suitable for the application (see later Fig. 5.2.2-4). A selection of available filters can be found at vendors, such as Mini-Circuit's Filter List, Farnell's Filter List or DigiKey Filters (SMA & Bandpass). It is alternatively possible to filter out undesired signals with a band-stop, high-pass and low-pass filter combination.

Table 3.2 – BPF Options

Device Name	Company	Price (£)	Lead Time	Technical Specification	URL
SXBP-707+	Mini-Circuits	22.70	Shipping	670MHz Centre Frequency (PB = 645-695MHz) 70dB out of band loss	SXBP-707+ (Mini-Circuits)
SXBP-640+	Mini-Circuits	22.70	Shipping	640MHz Centre Frequency (PB = 600-680MHz) 80 dB out of band loss	SXBP-640+ (Mini-Circuits)
RBP-650A+	Mini-Circuits	17.34	Shipping	652MHz Centre Frequency (PB=624-680MHz) 25 dB out of band loss	RBP-650A+ (Mini-Circuits)
BP2816A0660SNTR\50	Kyocera	24.25	Shipping	660 MHz Centre Frequency (PB = 520-800MHz) 38dB out of band loss	BP2816A0660SNTR-50 (DigiKey)
FI168B0845D9-T	Taiyo Yuden	0.65	Shipping	844 MHz Centre Frequency (PB = 729-960MHz) ~20dB out of band loss	FI168B0845D9-T (Mouser)
BPF-A730+	Mini-Circuits	45.47	Shipping	732MHz Centre Frequency (PB = 670-795MHz) 60dB out of band loss	BPF-A730+ (Mini-Circuits)

3.3 Low Noise Amplifier (LNA)

Both the target surveillance and reference channel require amplification to maximise the output signal-to-noise of processing. The maximum input of the USRP2954R is stated as -15dBm = 0.01mW. A 100kW transmitter (80dBm) placed 10km from the receiver will experience approximately 110dB of free-space losses at 700MHz (DVB-T). Thus, the power of the signal measured at the reference receiver channel will be -20dBm, assuming no other losses which there will be. At 30km, this will be -30dBm. For the surveillance channel there will be a longer propagation path, and a further reduction from the backscatter off targets of interest. Both of these channels can have their (filtered) signal amplified to maximise the dynamic range of captured returns, that will later improve the Signal-to-Noise Ratio (SNR) and thus operating range of the PCL device. It is however, absolutely essential not to overload the receiver with too strong a power to avoid damaging the device. An in-field measurement of the absolute power of received signals (with antenna gain, cable losses, other geographical factors etc.) will dictate the model of LNA required.

Again, these components are very common and fairly cheap at <1GHz, in particular at the target frequency bands of DVB-T, DAB, VHF or otherwise, see for example LNA List (Mini-Circuits), SMA-based LNA List (DigiKey)

Some candidate SMA-based LNAs suitable for a DVB-T system are shown in Table 3.3.

Table 3.3 – LNA Options

Device Name	Company	Price	Lead Time	Technical Specification	URL
ZRL-700+	Mini-Circuits	151.73	Shipping	Signal Gain >27dB, with 2dB Noise Figure (250-700MHz)	ZRL-700+ (Mini-Circuits)
ZRL-1200+	Mini-Circuits	151.73	Shipping	Signal Gain >24dB, with 2dB Noise Figure (650-1200MHz)	ZRL-1200+ (Mini-Circuits)
ZX60-112LN+	Mini-Circuits	89.76	Shipping	Signal Gain >16.5dB, with 1.2dB Noise Figure (400-1100MHz)	ZX60-112LN+ (Digi-Key)
ZFL-1000LN+	Mini-Circuits	118.51	Shipping	Signal Gain >16.5dB, with 2.9dB Noise Figure (0.1-1000MHz)	ZFL-1000LN+ (DigiKey)
TAMP-72LN+	Mini-Circuits	29.30	Shipping	Signal Gain 20dB, with 1.2dB Noise Figure (400-700MHz)	TAMP-72LN+ (Mini-Circuits)+

3.4 Antenna

Two antennas are required in the operation of a passive radar system – one each for the reference and surveillance channels. It is required only to connect SDR input to antenna via SMA, N-Type or other connector, with appropriate attenuation or amplification. It could be desirable to have a highly-directional reference antenna, and a less directional surveillance antenna in a scenario where the surveillance antenna has a fixed placement.

There exists the option to use a *Yagi-Uda* or *Patch* Antenna, with both schematically shown in Figure 3.5. Yagi-Uda antennas in-particular are commonly designed to receive signals of DVB-T and can typically be purchased from any hardware store.

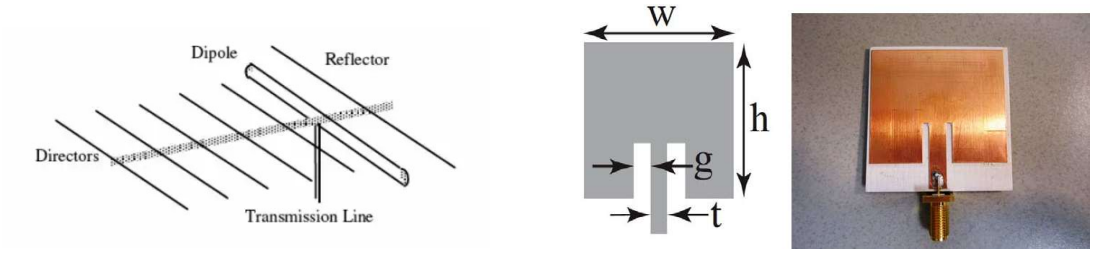

Figure 3.5 – Yagi-Uda (left) and Patch Antenna (right)

The choice of which of these antenna types can be largely considered a matter of convenience and operational setting. Table V (Yagi-Uda) and Table VI (Patch) list some antennas available from online retailers that would be suitable for the application. The specific model of choice will be dependant on the IoO frequency used, and within this is a choice of trade off with gain and directionality against coverage, which requires an assessment for optimal performance. The initial design will deploy Yagi-Uda antennas due to their higher directionality, which would be more indicative of a fielded system with an array of antennas (and hence high gain), however patch antennas are always an option and UoB have even built custom ones in the past.

Yagi-Uda	
Pros • Large Gain • Strong Directionality / Directivity 9dBi • Fairly Flat Frequency Dependency (flexible) • Optimal for HF to UHF (300MHz-1GHz)	Cons • As highly directional, line of sight to target/ transmitting station is more important • Requires a proper, fixed mount point, robust to weather

Table 3.5-1 – Yagi Antenna Options

Device Name	Company	Price	Lead Time	Technical Specification	URL
SV9354 (see Sec 5.1)	One-for-all	~40.00	Widely stocked	400-700MHz, 3/4/5G Filter, F-Type Female, Pole Mount	SV9354 (OfA)
BGYD890K	Amphenol PCTEL	84.01	14 weeks (if not in stock)	890-960MHz, Gain 10dBd, N-Type Female, Pole Mount	BGYD890K (DigiKey)
7175833	Amphenol Procom	339.03	5 Weeks	769MHz-896MHz, Gain 12.1dBi, N-type Female, Pole Mount	7175833 (DigiKey)

Patch Antenna	
Pros • Modest Gain • Good Directionality / Directivity 6dBi • As less directional, line of sight to target/ transmitting station can be more coarse • Less effort to fix flat antennas in mount, fixed mount point, robust to weather	Cons • Smaller Bandwidth, greater frequency dependency (less flexible) • Lower overall gain will reduce maximum detection range/size etc.

Table 3.5-2 – Patch Antenna Options

Device Name	Company	Price	Lead Time	Technical Specification	URL
ARRKP4065-S915A	Abracon LLC	11.39	25wks	902-928MHz, Gain 1.5dBi, Dielectric Ceramic	ARRKP4065-S915A (DigiKey)
FXP280.07.0100A	Taoglas Limited	12.36	6 wks	863MHz-870MHz, 1.5dBi, Flat Patch	931-1089-ND (DigiKey)
ANT-8/9-FPC-UFL-100	TE Connectivity Linx	3.67	6 wks	Dual Band, Flat Patch	ANT-8/9-FPC-UFL-100 (DigiKey)

4 Signal Processing Requirements

The signal processing utilised to enable PCL is described in this section. At first, Section 4.1 describes in words the signal processing steps to perform detection from the measured signals at the reference and surveillance channels. Section 4.2 will further describe the essential operations taking place to enable PCL. These steps were illustrated in Fig. 3, and now they will be further explained to how they enable PCL.

The USRP acquired will allow, at minimum, the (down-conversion, see Sec 4.1.1), formatting and recording of gathered data to disk. This can be performed with USRP compatible software such as NI's LabVIEW, MatLab's Radio Support ToolBox or Open Source GNU Radio.

From this point, off-line processing of gathered data will be the approach for determining the performance of the system. At first, the algorithms described in this section will be implemented within a standard programming language (MatLab or Python) to confirm the operation of the algorithm for the data collected in field recorded with the USRP. This subsequently will provide a flexible environment for analysing performance of the system under different operational conditions (such as, a different choice of reference IoO or different control targets, coherent processing duration), allowing a clear presentation of system performance results as function of key operational parameters. The required signal processing to perform detection, range and velocity measurements are described in 6 steps.

1. Down-conversion of received signals at their electromagnetic carrier frequency to baseband.
2. (Digital) Fourier Transform of both the reference and amplified, filtered surveillance signal.
3. Mix (multiply) these together for each sample with time-reversal and complex conjugation of one of the signals.
4. Perform the Inverse Fourier Transform on this result to compress the signal and discretisation into range samples

(NB: This procedure 1 to 3 can be referred to as taking the *cross-correlation* of two signals. This produces a range signal for a set operational timestep. The frequency of these samples occurs normally at the signal bandwidth.)

5. Collecting and storing these (slow-time) samples, allows a final FFT in the time axis to convert a timeseries signal per range gate into a range-Doppler map.
6. Detection via a suitable CFAR algorithm will produce detections at a fixed, desired rate of false alarm.

4.1 Description of Processes

Sec. 4.1.1 explains how the USRP processes the received signal (modulated into the carrier frequency) into baseband samples

Sec. 4.1.2 details steps 2-4 above; how a target's range is determined in PCL using the cross-correlation function.

Sec. 4.1.3 explains step 5 how a target's velocity is extracted from a consecutive series of measurements.

Sec. 4.1.4 explains step 6: how and why the CFAR algorithm will enable robust detection of targets.

4.1.1 Signal down-conversion to baseband

The first step occurs within the USRP / SDR to both channels simultaneously. The received signals at ~700MHz cannot be sampled by the USRPs ADC while satisfying the Nyquist sampling criteria, so it is *down-converted* to baseband before any further processing or recording. This is performed by mixing (multiplying) the received signal with a new signal at the same carrier frequency, which would be the ~700MHz signal.

Figure 4.1.1 illustrates this approach for a received signal oscillating over time, t, at its carrier frequency, f_0. Multiplying the received signal at carrier frequency, $\cos(f_0 + \phi)$, with itself, $\cos(f_0)$, yields two outputs according to the cosine trigonometric formula,

$$2\cos(A)\cos(B) = \cos(A - B) + \cos(A + B)$$

$$\therefore\ 2\cos(f_0 + \phi)\cos(f_0) = \cancel{\cos(2f_0 + \phi)} + \cos(\phi)$$

^twice carrier term removed by Low Pass Filter (LPF), leaving only the phase offset at baseband as the output.

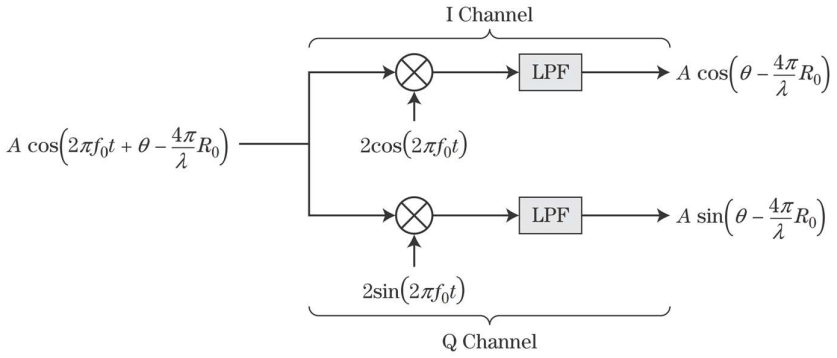

Figure 4.1.1 – Down-conversion of a received signal (at f_0, carrier frequency) to two orthogonal baseband signals, with the carrier frequency removed. From Chapter 8 of [2].

The signal oscillation at $2f_0$ is removed by low pass filter, returning only a signal at baseband. This is done similarly with an orthogonal signal, $\sin(f_0)$, to produce another, orthogonal baseband signal. The two orthogonal signals output allow representation of the signal as a complex value, with an amplitude and phase. Additionally, if only one of the outputs were used, it would be ambiguous to what direction the oscillation is occurring, which is directly related to the direction of travel of a detected target. This output is the In-phase/Quadrature (I/Q) output, that is the raw data representation of radar signals that are subject to all further processing.

4.1.2 Range Compression

The PCL system will receive two signals at the Reference, (R), and surveillance (S) channels. $R(t)$ and $S(t)$ are complex signals measured by the receiver.

The form of $R(t)$ received signals will be an intricate timeseries pattern that is transmitted by the IoO, along with any interference caused by multipath, diffraction and noise. For DVB-T, the

waveform transmitted is well defined, with the contents of the programme digitally scrambled and appearing noise-like with a flat-top frequency distribution [1].

$S(t)$ contains $R(t)$ but with a delay (due to the greater propagation path length after reflection off the target) and weaker, (due to the small size of the target). This delay is not known a priori but will be found and subsequently used to declare target range.

As $S(t)$ contains a copy of $R(t)$, if we find a delay value, τ, for which $S(t)$ and $R(t)$ are the most similar ($S(t) \approx R(t-\tau)$), then we have determined the delay. This is achieved using a cross-correlation operation between these two signal channels.

$$A(\tau) = \text{Cross-Correlation}(\, S(t), R(t)\,) \quad \equiv \quad S(t) \star R(x) \equiv (S \star R)(\tau) \quad = \int_{-\infty}^{\infty} S(\tau)^* R(t+\tau)\, dt$$
$$\equiv \int_{-\infty}^{\infty} S(t-\tau)^* R(t)\, dt$$
$$= FT^{-1}\,(\, FT(f(-t)^*) \cdot FT(g(t))\,)$$

Where * (asterisk) indicates the complex conjugate, and τ is a variable conceptually representing a time delay between the two signals. This outputs a new 1-D vector as a function of τ, $A(\tau)$. The cross-correlation is performed by Fourier Transforming (FT) each of the signals, after time-reversing and complex conjugating one of them, mixing (multiplying) them, and finally performing and Inverse FT (FT^{-1}). This approach is more computationally efficient, and is possible thanks to the convolution theorem. Target reflections of the IoO signal will lead to peaks at values of τ that correspond to the delay of the received signal, from which the target range is determined with the knowledge of the speed of light. This process is illustrated in Figure 4.1.2.

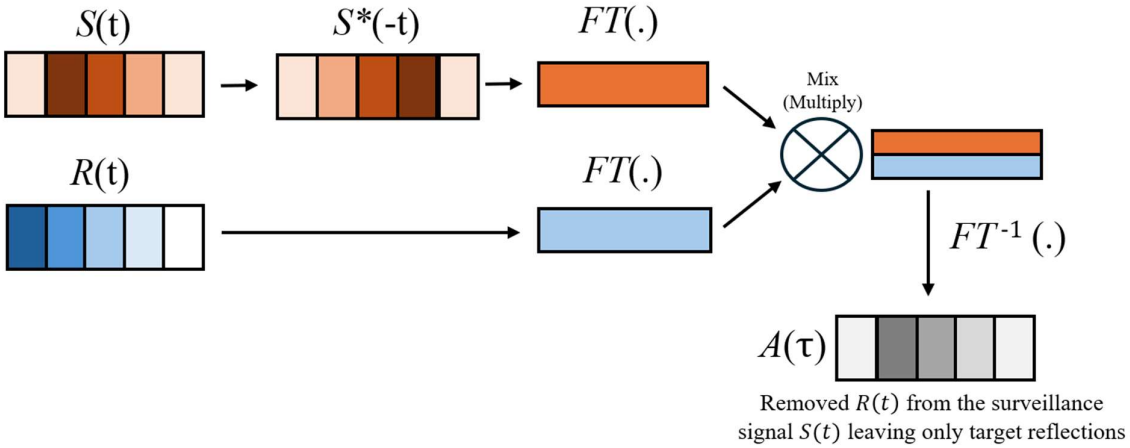

Figure 4.1.2 – Illustration of cross-correlation steps to isolate target reflection induced delays from the reference channel.

This 1-D vector output is a function of delay, τ. The strength of each discrete sample along τ indicates the presence of signal of increased received power at the delay value. If multiple targets are present at different delays, they will appear in the *range profile* at with their delay after matching to the reference signal.

4.1.3 Velocity Measurement

After producing $A(\tau)$ for a recorded sample of $S(t)$ and $R(t)$, velocity information can be garnered by considering a sequence of consecutive measurements, $A_0, A_1 \ldots A_{N-1}$, where N is the number of samples to be coherently processed.

For a target at $\tau = \tau$, its complex value will have a magnitude depending on the reflected strength from the target, and a phase that is dependent on the initial phase from the IoO transmitter, the propagation path length and EM frequency.

If the target, between A_n and A_{n+1}, moves towards/away from the surveillance channel, the path length will have decreased/increased, and so the phase of this sample will have changed due to both the target's location and the passing of time. For a series of collected samples of $A_0, A_1 \ldots$, the change of measured phase is capturing the Doppler shift of the signal caused by target motion.

An FFT across consecutive $A_0, A_1 \ldots$ samples after conversion to baseband will yield peaks at frequencies corresponding to the Doppler shift imparted by the target. This is referred to as *coherent integration* of multiple pulses. This both increases the SNR of returns and allows velocity of measurement of targets that otherwise may be obscured by returns caused by static clutter, such as terrain or buildings. Figure 4.1.3 illustrates this process for using consecutive A_n measurements to construct a range-Doppler map. The extent of the velocity axis is the Pulse Repetition Frequency (PRF), which is effectively the rate of capture of $A(\tau)$.

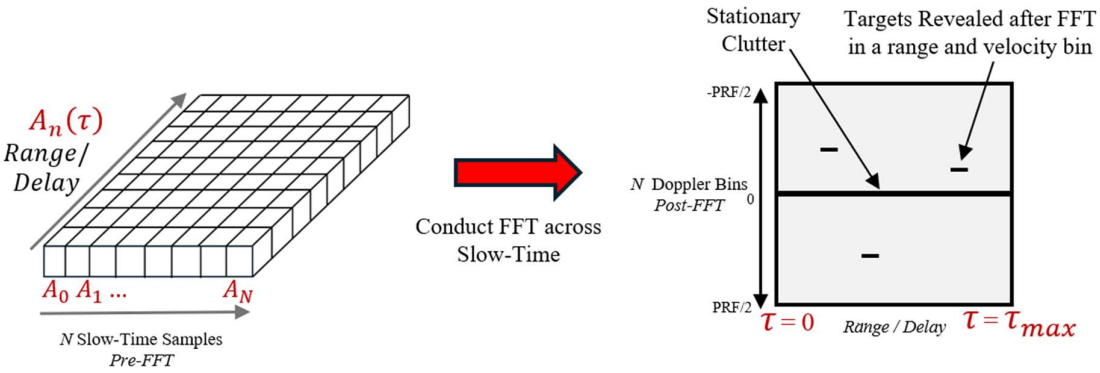

Figure 4.1.3 – FTT on collection of $A_0 \ldots A_N$ to provide a range-Doppler map with moving targets and stationary clutter

The value N to an extent dictates the performance of the radar. A larger N means more samples are coherently integrated, which leads to a finer Doppler resolution (more and narrower velocity bins for the same velocity swath), and greater power of genuine signals provided it is not rapidly accelerating. A larger N means a greater SNR of target returns, thus a greater operational range, but also a larger time duration over which returns are integrated, so reducing the update rate.

If a target is rapidly accelerating, then returns will not be integrated totally coherently so the resultant target peak will less than optimal, and will be spread over numerous Doppler bins.

Further, if the reflected power off the target, (its Radar Cross Section (RCS)) is significantly fluctuating, then it is not a coherent scatterer and will suffer additional loss of integration gain. RCS will vary depending on the target's orientation relative to the receiver, or if there are

changes of the target in flight that cause a change in its RCS over time. This phenomena is mathematically described in the Swirling model statistical framework [3]. Knowledge or analysis of the nature of target scattering and coherency at the operational frequency will assist in optimizing the coherent integration length, N, for different targets.

In conclusion, to allow the consistent detection of highly manoeuvrable targets, N must not be set excessively large. The optimal value of N will depend on many factors (target type, scattering nature, acceleration) and will require experimentation to assess the detectability of specific targets in any PCL setting.

4.1.4 Target Detection

The collection and coherent integration of a sequence of $A_0 \rightarrow A_{N-1}$ leads to the production of a *range-Doppler map* from which a target detection algorithm can be implemented.

A target detector sets a threshold of signal power across the range-Doppler map. The three possible outcomes of this approach are:

1. Correct Decision: A detection is declared for a target that exists
2. False Alarm: A detection is declared for a target that does not exist
3. Missed Detection: No detection is declared for target that exists

False alarms occur when a source of non-target source of noise or interference causes a resolution cell of a range-Doppler map to be greater than expected. A detection may be missed if the power of its signals are not sufficiently strong or coherent (target accelerating too fast) to be integrated above the noise floor.

Naturally, the minimisation of false alarms and missed detections improves the operational standard of the PCL or radar in general. Raising the detection threshold means less chance of false alarms and increases the chance of missed detections.

In radar to combat this fundamental trade-off, the standard detection algorithm is Constant False Alarm Rate (CFAR) thresholding.[1] The working principle is to update the threshold such that the Probability of False Alarm (P_{FA}) is constant across time and space, allowing for the interference to change over time and space.

Figure 4.1.4 illustrates the CFAR principle via an expression of the probability distribution function of interference and noise, and a target within interference and noise.

[1] AKA Neyman-Pearson detector. Variations of CFAR exist, (Cell-Averaging, Order Statistics, Greatest-of, Least-of), and additionally, deep learning based detection is a modern research trend. CFAR however, is the work horse of radar detection in almost all scenarios.

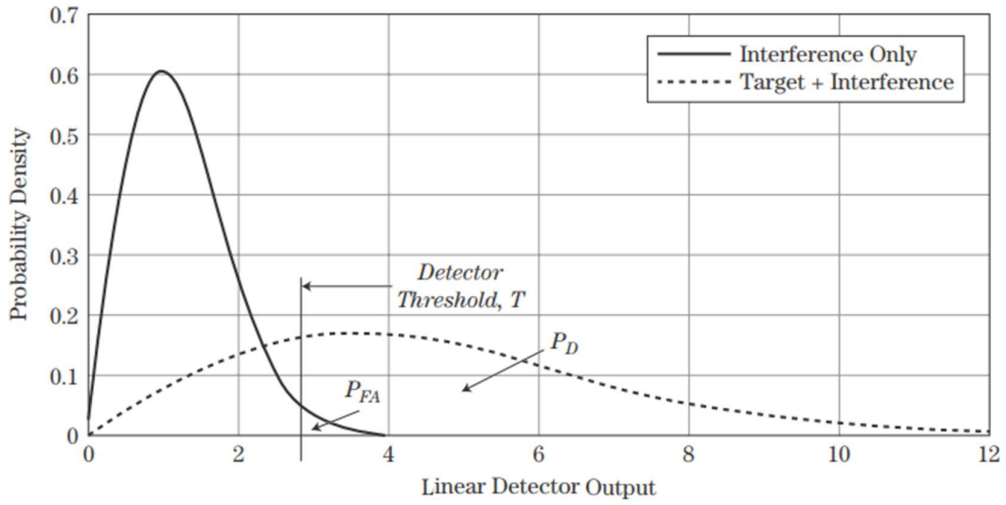

Figure 4.1.4 – CFAR Principle. 'Linear Detector Output' describes a range Doppler map that uses the (linear) magnitude of the complex vectors to represent power. From Chapter 16 of [2].

For the majority of the range-Doppler map, target presence will not exist, and the power in each range and Doppler bin will be dictated by present noise and interference. This distribution can be measured, and is shown in Fig. 4.1.4 as the solid black line.

Then on top of this, a target will introduce additional signal power to any existing thermal or interference noise. The dotted line of Fig. 4.1.4 represents a possible distribution of an arbitrary target.

The CFAR system sets the threshold such that the area under the curve due to the target-less power probability distribution *above the threshold* is constant. A value such as $P_{FA} = 10^{-4}$ may be used, which is 1 false alarm per 10,000 observations. In real terms, a *False Alarm Rate (FAR)* for a system can be declared, mathematically expressed as:

$$FAR = \frac{P_{FA}M}{T_M} = N_D P_{FA}$$

where M is the total number of resolution cells for each coherently processed batch of returns, and T_M is the rate of returns processed i.e. how many range-Doppler maps are produced per second. Inspection of FAR allows operators to set the rate of false alarms they are happy to deal with for their system deployment.

With the P_{FA} set constant, the performance of the radar in terms of Probability of Detection (P_D) can be assessed and presented as a key performance metric of the system. Typically, this is shown as a Receiver Operating Characteristic (ROC) curve with P_{FA} on the x-axis and P_D on the y-axis [4]. The area under this curve reflects the quality of detector performance. Different target SNR values can be assessed against a ROC curve, which can help an operator choose the value of P_{FA} that best suits their system and anticipated targets.

5 Site Assessment

The ultimate PCL deployment site is at the Kryoneri Observatory in the Corinth District of Greece. At UoB, remote preparations are underway to understand how the deployment on-location will be shaped, based on realities of the existing IoO infrastructure. There are unknown factors at the deployment site that will require an on-location assessment and the major of these is which DVB-T transmitter in the region is optimal to use and what are its expected power levels.

To ensure we are able to rapidly conduct the deployment, we first are to prepare the instrumentation that will be used at the Kryoneri site, with initial testing at UoB where local IoO parameters readily accessible and better known. This will allow confidence to declare the expected performance at the Kryoneri site, where there are presently many unknowns related to the IoO, and how other factors such as geography will affect the quality of the direct signal.

This section is divided into two subsections. The first, Section 5.1, shows an example power measurement of a DVB-T transmitter located 17km from the measurement site at the University of Birmingham (UoB). Then, Section 5.2 shows a remote assessment of the Kryoneri Site considering known IoO locations, and available information, that with some assumptions allows us to estimate the operational range of the proposed PCL system.

5.1 UoB Transmitter Measurement and Assessment

A DVB-T transmitter tower at 200kW based in Sutton Coldfield is located 17.44km from UoB, as shown in Figure 5.1-1.

Fig. 5.1-1 – Distance from Sutton Coldfield Transmitting Station to UoB

Key differences between this scenario and the one at Kryoneri (see Sec. 5.2 following) are:

- Greece is an extremely mountainous landscape, which will effect the signal propagation from the IoO. Contrastingly, Birmingham is fairly flat but much more urban, which will have a different but similarly detrimental effect.
- The Sutton Coldfield transmitting station was known to operate with 200kW of output power. The power of transmitters in Greece is not known.

Using a spectral analyser (Rhode & Schwarz FSH6, Figure 5.1-2 (a)) and a CotS Yagi-Uda antenna (Figure 5.1-2 (b)) for DVB-T reception, the measured signals allows an assessment of the direct signal, which in turn allows a deeper assessment of the ability to perform PCL target measurements.

a) Rhode & Schwarz FSH6 Spectral Analyser

b) Gisbert-Kapp Roof top with SV9354 Yagi-Uda

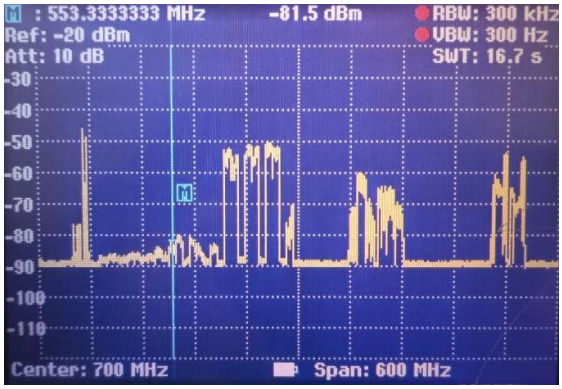

c) Spectra @ 250MHz – 1.1GHz

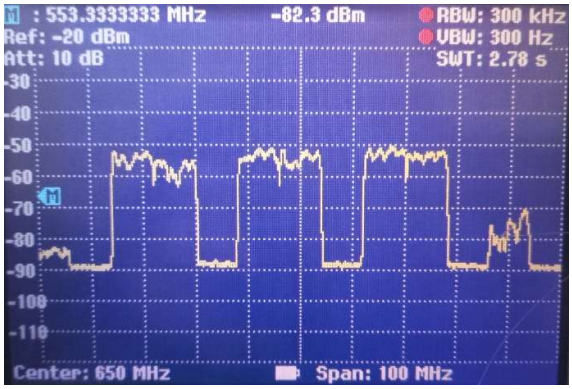

d) Spectra @ 600-700MHz (DVB-T Signals)

Figure 5.1-2 – Measurements at VFH with FSH6 Spectral Analyser

The signals on display in Figure 5.1-2 (c) and (d) demonstrate the expected returns that will aid in the component choice to optimise the PCL system prior to its construction. Fig. 5.1-2 (c) shows the measured signals between 250MHz and 1.1GHz, with three strong and distinct DVB-T signals just to the left of centre [1], [5]. Fig. 5.1-2 (d) is zoomed into these signals showing a 100 MHz span at centre frequency, 650MHz.

The DVB-T signals are clearly visible, and as expected their bandwidths are ~7MHz. Their centre frequency are easily read, and match the existing OFCOM (Office of Communications, UK telecommunications regulatory authority) publicly available values (see the Digital Television Table). Each flat top return is in fact two adjacent Orthogonal Frequency-Division Multiplex (ODFM) channels.

5.2 Kryoneri Site Transmitter Assessment

5.2.1 IoO Infrastructure

Since 2006, freeview DVB-T channels from the state broadcaster ERT have been in operation [6], with Digea in 2009-2015 setting up a total of 156 transmitting sites set up near population zones. The available coverage using DVB-T is detailed on the Digea website (see Section 5.2.2 following).

5.2.2 DVB-T Transmitter Locations

Using the Digea site's Coverage Checker for the Kryoneri location for TV reception, it is recommended to tune into the transmitters at sites: *Ymittos, Osios Patapios,* or *Parnitha*. Figure 5.2.2.1 shows the simulated coverage as provided by Digea.

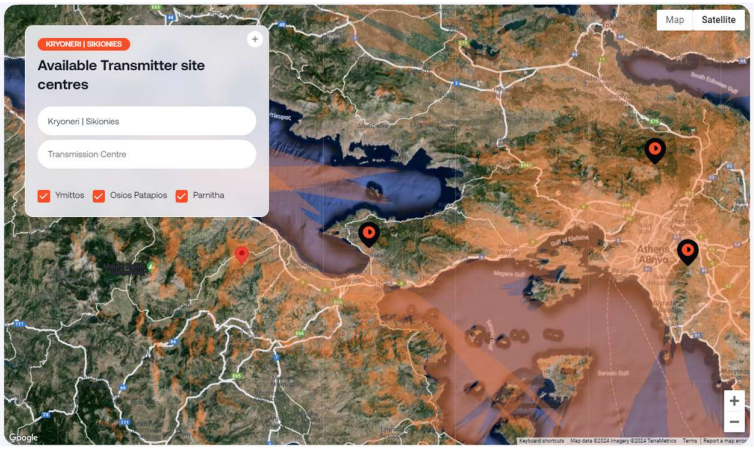

a) Three Transmitter Stations recommended by Digea

b) *Osios Patapios* simulated coverage

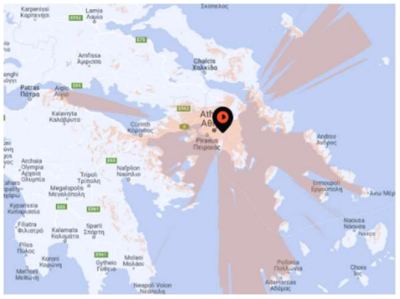

c) *Parthina* simulated coverage

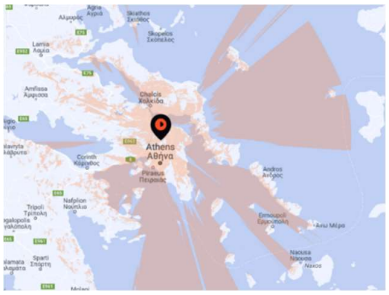

d) *Ymittos* simulated coverege

Figure 5.2.2-1 – Digea Coverage Recommendation for TV reception at Kryoneri Observatory Site.

Osios Patapios, is 31.1 km from where the surveillance channel will be. The others, based near Athens, are ~100km away from the observatory, which is a very long distance and thus will experience a an extra 10dB of free space path loss, with further unknown complications arising from line of sight, diffraction and reflections.

Other IoO transmitters exist in the region, and are candidates for gathering the surveillance signal. Figure 5.2.2-2 shows the 14 closest Transmitters, and Fig 5.2.2-3 shows the three closest of these that will likely provide the best reference signal. *Xylokastro* and *Nemea* were not listed as options on the Digea site, but with a suitably tall mast their signals could conceivably be the best choices for PCL. There is no choice but to perform our own measurements to determine the best transmitter(s) to enable robust PCL for the specific site, as the prescription is ultimately for TV reception and not PCL feasibility.

Of the three transmitters in Figure 5.2.2-3, each of them broadcast the same channels shown in Figure 5.2.2-4. This may lead to some difficulty in supressing the unreferenced IoOs, but beneficially provides a redundancy of transmitter that will allow the same hardware to be used for the three different directions these three transmitters are oriented.

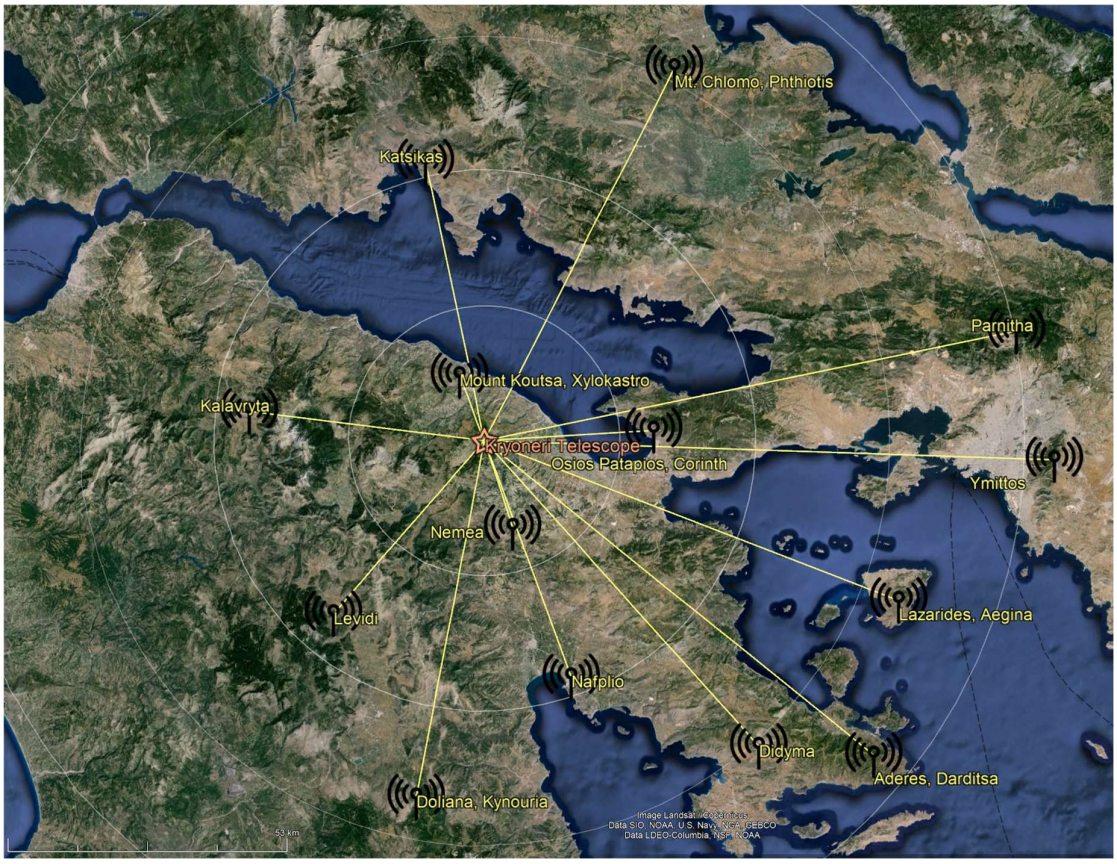

Figure 5.2.2-2 – Locations of possible IoOs listed by Digea.[2]

[2] White circles in these figures show the distance from Kryoneri Observatory in 25km range increments.

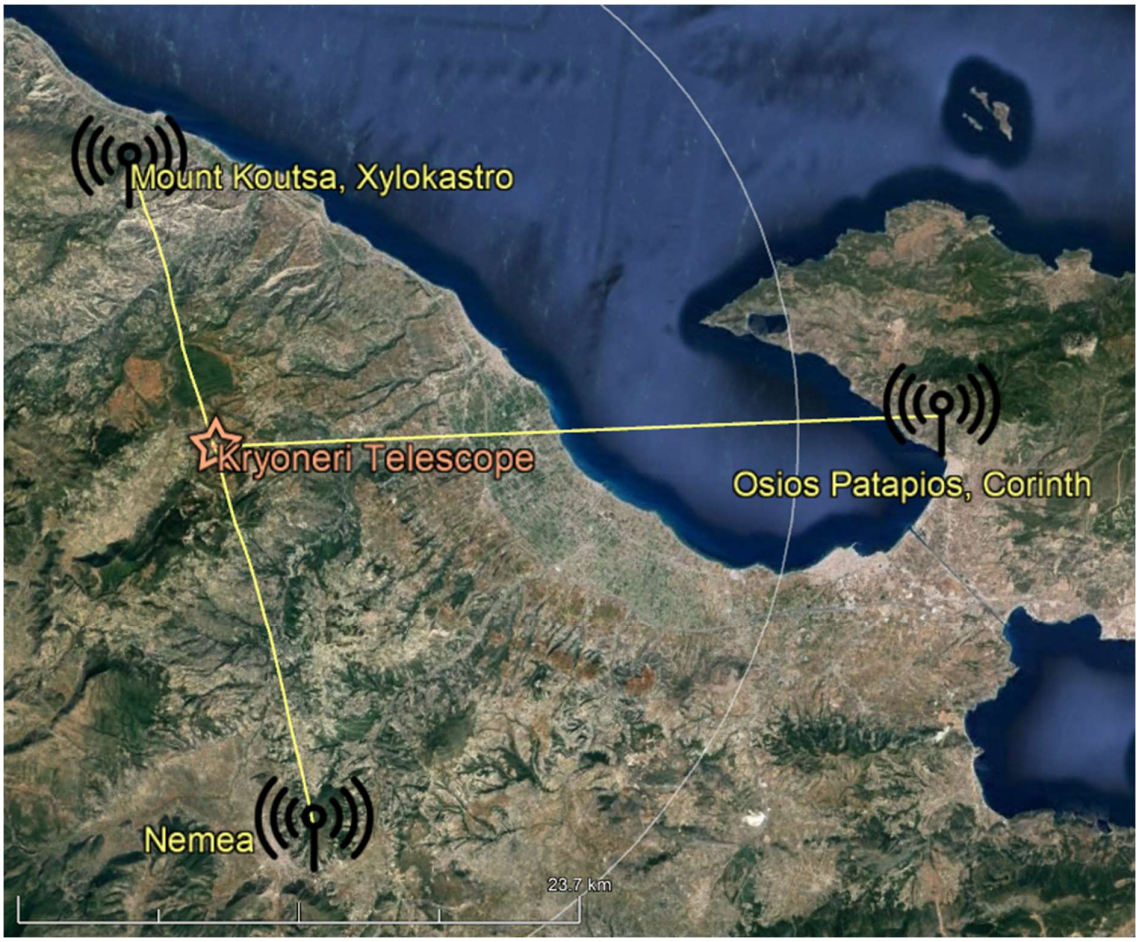

a) Three closest transmitter locations

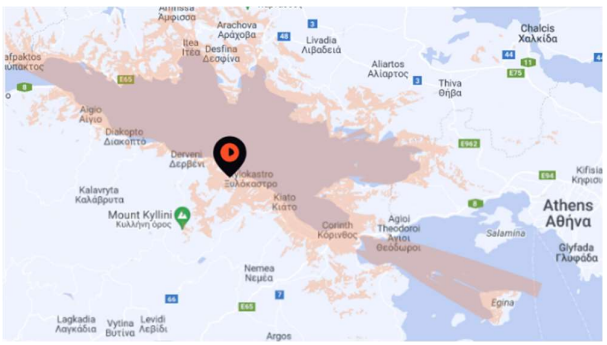

b) *Xylokastro* simulated coverage map

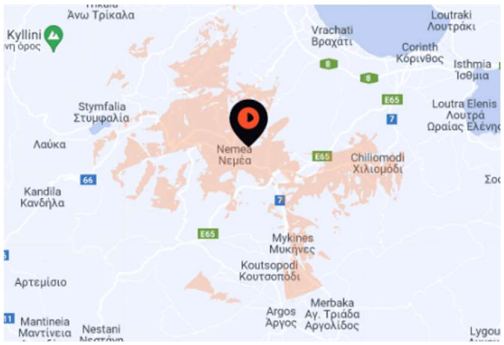

c) *Nemea* simulated coverage map

Figure 5.2.2-3 – Closest Candidates for IoO surveillance signal:
Xylokastro, Nemea and *Osios Patapios*

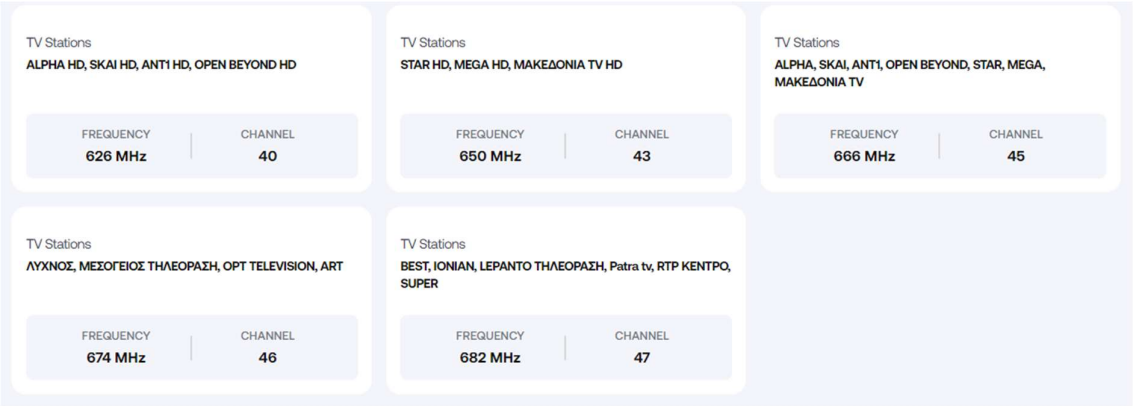

Figure 5.2.2-4 – Channels/Frequencies broadcasted by each of the three closest, candidate transmitters.

5.2.3 First DVB-T PCL Range Assessment

The operational range of the PCL system can be estimated using the bistatic Radar Range Equation (RRE) [2], [5]. This equation models each component of the target, transmitter, receiver and length scales of a radar scenario, and regularly presented in the following form yielding SNR,

$$SNR = \frac{P_T\, G_T\, G_R\, \lambda^2\, \sigma_{RCS}\, T_{Processing}}{(4\pi)^3\, R_T^2\, R_R^2\, k_B T_0 FL}.$$

The transmitter parameters of this equation are either acquired or estimated – with an in situ measurement allowing confirmation of estimations. The receiver parameters are known more precisely based off the USRP-2954's specifications, but will benefit from a laboratory confirmation upon completing the hardware setup. The transmitter power is usually expressed in terms of EIRP (Equivalent Isotropic Radiated Power) = $P_T G_R$, which expresses the total power needed for an equivalent isotropic antenna. Upon arrival at the Kryoneri site, this is how we will characterise the transmitting IoO our application is dependent on.

Table 5.2.3 – Parameters and values of the radar range equation[3]

Symbol	Parameter (Unit)	Value	Comment
P_T	$Power\ of\ Tranmsitter\ (W)$	50x10^3	Within 10 and 200
G_T, G_R	$Gain\ of\ Transmitter, Reciver\ (dB)$	4 ~6	USRP-2954 + YagiUda
λ	$Operating\ Wavelength\ (m)$	0.462	
σ_{RCS}	$Radar\ Cross\ Section\ (dBm^2)$	Drone/Bird ≈ -20 Aircraft ≈ +10	Depends on the Target [7]
R_T, R_R	$Target\ Range\ to\ Trans., Recei.\ (m)$		
k_B	$Boltzmann's\ Constant\ (W\ s\ K^{-1})$	1.38x10^{-23}	
T_0	$Standard\ Temperature\ (K)$	290	
F	$Noise\ Figure\ (dB)$	6	USRP-2954 Spec.
L	$System\ Losses\ (dB)$	~10	Cable Loss etc.
$T_{Processing}$	$Coherent\ Processing\ Time\ (s)$	0.5	0.5 Second integration, using PRF 1kHz (per Sub-Frame)

[3] Dimensionless units are expressed as dB. Value column cells are darkened for values estimated at the present time, requiring a site visit / evaluation based of measurements at the site.

These listed parameters allow for an initial illustration of anticipated system performance. Figure 5.2.4-1 shows the solving of the RRE to overlay the targets calculated SNR on map of the receiver and transmitter locality, using the parameters in Table 5.2.3, the *Osios Patapios* transmitter location, and an aircraft target (+10dBm^2) 10000m above sea level.

The plot showcases '*Ovals of Cassini*', where the strongest signal occurs closest to the receiver and transmitter. This is due to the inverse square fall of signal in range. Another trade off presents itself – the closer the receiver and transmitter, the better the direct reference signal will be, but the extent of coverage will be slightly reduced due to this physical phenomenon.

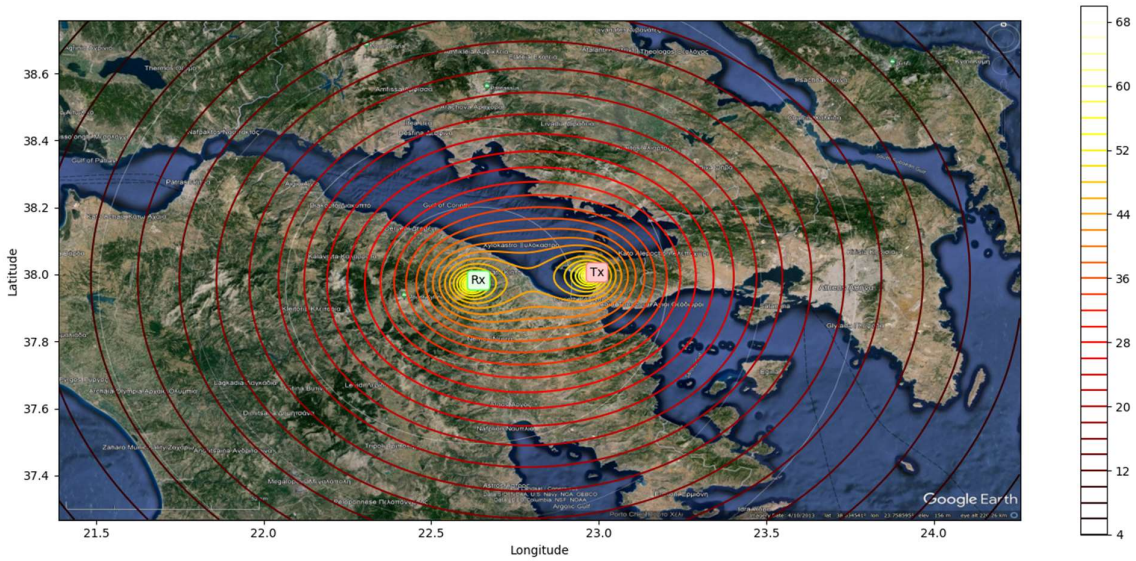

Figure 5.2.4-1 – SNR Contour of Target Location with *Osios Patapios* transmitter location and otherwise estimated parameters, considering a aircraft target at 10000m altitude.

A SNR of +20dBs can be used as a very strict criterion for reliable detection performance as a starting point. With more information of the transmitter, and chosen signal processing, estimations of maximum operational range can be calculated and tested against real observations to allow a precise prediction of future modification to the system.

Figure 5.2.4-2 shows the region that a target, using the estimated parameters in Table 5.2.3, for a drone target (assumed radar cross-section of -20dBm^2) at 900m altitude in (a), and a medium aircraft target (+10dBm^2) at 10,000m altitude in (b). The aircraft result (b) showcases that there is additional range to the receiver site if the target is in the direction of the IoO transmitter.

a) Drone target (-20dBm^2) at 900m altitude.
Distance from target to receiver (radius of white dashed line): 5.09km

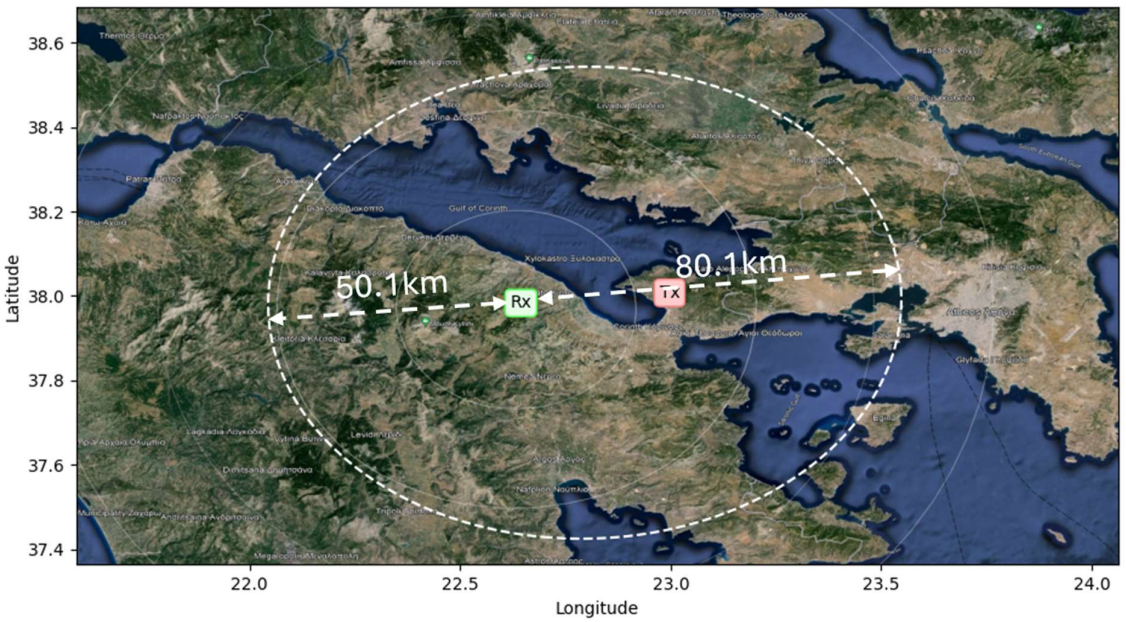

b) Aircraft target (+10dBm^2) at 10000m altitude.
Min. distance to receiver, 50.10km; max. distance, 80.1km

Figure 5.2.4-2 – Estimated 20dB limits of detection

6 References

[1] J. E. Palmer, H. Andrew Harms, S. J. Searle, and L. M. Davis, "DVB-T passive radar signal processing," *IEEE Trans. Signal Process.*, vol. 61, no. 8, pp. 2116–2126, 2013, doi: 10.1109/TSP.2012.2236324.

[2] M. A. Richards, J. A. Scheer, and W. A. Holm, *Principles of modern radar: Basic principles*, vol. I. 2010. doi: 10.1049/sbra021e.

[3] C. G. Soriano and N. C. Ferry, "Algorithms to Generate Random Samples following the Swerling Models," 2019. [Online]. Available: https://api.semanticscholar.org/CorpusID:204914365

[4] A. Asif and S. Kandeepan, "Cooperative fusion based passive multistatic radar detection," *Sensors*, vol. 21, no. 9, 2021, doi: 10.3390/s21093209.

[5] H. Griffiths and C. J. Baker, *An Introduction to Passive Radar*. Artech House Publishers, 2017.

[6] D. A. Kateros *et al.*, "DVB-T network planning: A case study for Greece," *IEEE Antennas Propag. Mag.*, vol. 51, no. 1, pp. 91–101, 2009, doi: 10.1109/MAP.2009.4939022.

[7] A. F. Association, "B-2 at 30: Improving with Age," *Air Force Mag.*, vol. 102, no. 7, pp. 33–35, 2019.